Frontiers of Information Technology & Electronic Engineering
www.jzus.zju.edu.cn; engineering.cae.cn; www.springerlink.com
ISSN 2095-9184 (print); ISSN 2095-9230 (online)
E-mail: jzus@zju.edu.cn

Supplementary materials for

Yunpu ZHANG, Qiang FU, Ganlin SHAN, 2023. A multi-sensor-system cooperative scheduling method for ground area detection and target tracking. *Front Inform Technol Electron Eng*, 24(2):245-258.
https://doi.org/10.1631/FITEE.2200121

1 Target-tracking algorithm

The purpose of moving target tracking is to estimate the target state at each time step. For target n, the expectation and covariance matrices of its state estimation at time step k are denoted as $\hat{\boldsymbol{X}}^n_{k|k}=\left[\hat{x}^n_{k|k},\hat{\dot{x}}^n_{k|k},\hat{y}^n_{k|k},\hat{\dot{y}}^n_{k|k}\right]^{\mathrm{T}}$ and $\boldsymbol{P}^n_{k|k}$, respectively.

For the off-road target, whose motion is not influenced by road constraints and for which the motion model set $\boldsymbol{\eta}^n_{\mathrm{model},k}$ is fixed, we apply the interacting multiple model (IMM) and cubature Kalman filter (CKF) algorithm to track it (Xu et al., 2019).

For the on-road target, the motion model is related to the road segment where it is located. Therefore, its motion model set $\boldsymbol{\eta}^n_{\mathrm{model},k}$ is time-varying and cannot be tracked by the IMM algorithm. To solve this problem, we introduce the variable-structure interacting multiple model (VS-IMM) algorithm (Kirubarajan and Bar-Shalom, 2003; Yu et al., 2016), in which the model set can be updated adaptively and the target state is then estimated based on the IMM algorithm. As explained in Section 4.2, the motion model of the on-road target at each time step is determined by the road segment where it is located, and the motion model is updated when the road segment has changed. Hence, we design an updated motion-model-set strategy based on the target state.

First, we judge whether the target is located at an intersection based on Eq. (S1):

$$\left[x_{\mathrm{inter}}-\hat{x}^n_{k-1|k-1},y_{\mathrm{inter}}-\hat{y}^n_{k-1|k-1}\right]\widehat{\boldsymbol{P}}^n_{k-1|k-1}\begin{bmatrix}x_{\mathrm{inter}}-\hat{x}^n_{k-1|k-1}\\ y_{\mathrm{inter}}-\hat{y}^n_{k-1|k-1}\end{bmatrix}\le\chi, \tag{S1}$$

where $\left(x_{\mathrm{inter}},y_{\mathrm{inter}}\right)$ are the coordinates of intersection, $\widehat{\boldsymbol{P}}^n_{k-1|k-1}$ is the position component of $\boldsymbol{P}^n_{k-1|k-1}$, and χ is the gate threshold of the Mahalanobis distance.

Then, the motion-model set is updated in the following three cases, depending on the location of the target. Fig. S1 shows the diagrams of the three cases.

Case 1 The road segment where target n is located at $k-1$ is the same as that at $k-2$.

This case indicates that the model set remains unchanged, that is, $\boldsymbol{\eta}^n_{\mathrm{model},k-1}=\boldsymbol{\eta}^n_{\mathrm{model},k-2}$.

Case 2 The road segment where target n is located at $k-1$ is different from that at $k-2$.

In this case, the model set should be updated, all the models are deleted from $\boldsymbol{\eta}^n_{\mathrm{model},k-2}$, and the model corresponding to the current road segment is added in $\boldsymbol{\eta}^n_{\mathrm{model},k-1}$.

Case 3 Target n is located at the intersection of multiple road segments.

In this case, the model set should be updated, all the models are deleted from $\boldsymbol{\eta}^n_{\text{model},k-2}$, and the models corresponding to all road segments connected to the intersection are added in $\boldsymbol{\eta}^n_{\text{model},k-1}$.

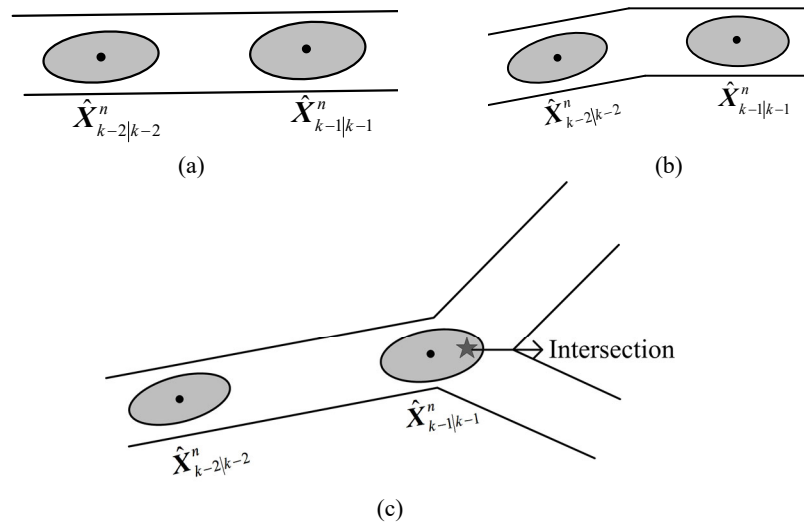

Fig. S1 Diagrams of three target location cases: (a) case 1; (b) case 2; (c) case 3

After updating the model set, the IMM algorithm can be used to estimate the on-road target state in the same way as the off-road target state.

However, due to the presence of the Doppler blind zone, the measurement of the target may not be achieved by the multi-sensor system. At this point, the measurement update cannot be performed in the filter, and the target state can be predicted only through the motion model, that is,

$$\begin{cases} \hat{\boldsymbol{X}}^n_{k|k} = \sum_{i=1}^{\eta_{\text{total}}} \mu^i_k \hat{\boldsymbol{X}}^{i,n}_{k|k}, \\ \boldsymbol{P}^n_{k|k} = \sum_{i=1}^{\eta_{\text{total}}} \left\{ \mu^i_k \left[\left(\hat{\boldsymbol{X}}^n_{k|k} - \hat{\boldsymbol{X}}^{i,n}_{k|k} \right) \left(\hat{\boldsymbol{X}}^n_{k|k} - \hat{\boldsymbol{X}}^{i,n}_{k|k} \right)^{\mathrm{T}} + \boldsymbol{P}^{i,n}_{k|k} \right] \right\}, \end{cases} \tag{S2}$$

with

$$\begin{cases} \hat{\boldsymbol{X}}^{i,n}_{k|k} = \tilde{\boldsymbol{X}}^{i,n}_{k|k-1} = \boldsymbol{F}^n_{\eta_k=i} \hat{\boldsymbol{X}}^{i,n}_{k-1|k-1}, \\ \boldsymbol{P}^{i,n}_{k|k} = \boldsymbol{P}^{i,n}_{k|k-1} = \boldsymbol{F}^n_{\eta_k=i} \boldsymbol{P}^{i,n}_{k-1|k-1} \left(\boldsymbol{F}^n_{\eta_k=i} \right)^{\mathrm{T}} + \boldsymbol{\Gamma}^n_i \boldsymbol{Q}_{\eta_k=i} \left(\boldsymbol{\Gamma}^n_{\eta_k=i} \right)^{\mathrm{T}}, \end{cases} \tag{S3}$$

where η_{total} is the total number of motion models, μ^i_k is the probability of model i at k, $\left(\hat{\boldsymbol{X}}^{i,n}_{k|k}, \boldsymbol{P}^{i,n}_{k|k} \right)$ is the state estimation under model i at k, and $\left(\tilde{\boldsymbol{X}}^{i,n}_{k|k-1}, \boldsymbol{P}^{i,n}_{k|k-1} \right)$ is the corresponding state prediction.

2 Posterior Carmér-Rao lower bound

PCRLB is also the inverse of the corresponding Fisher information matrix. According to Song et al. (2019), PCRLB of target n satisfies

$$E\left\{\left[\hat{\boldsymbol{X}}_{k|k}^{n}-\boldsymbol{X}_{k}^{n}\right]\left[\hat{\boldsymbol{X}}_{k|k}^{n}-\boldsymbol{X}_{k}^{n}\right]^{\mathrm{T}}\right\}\geq \mathbf{PCRLB}_{k}^{n}=\left(\mathbf{Fisher}_{k}^{n}\right)^{-1}, \tag{S4}$$

where $\mathbf{PCRLB}_{k}^{n}$ and $\mathbf{Fisher}_{k}^{n}$ are the PCRLB and Fisher information matrix of *n* at *k*, respectively.

Assuming that sensor *m* is activated to track target *n* at *k*, $\mathbf{Fisher}_{k}^{n}$ can be obtained by recursion, that is,

$$\mathbf{Fisher}_{k}^{n}=\boldsymbol{D}^{22}\left(\boldsymbol{X}_{k-1}^{n}\right)-\boldsymbol{D}^{21}\left(\boldsymbol{X}_{k-1}^{n}\right)\left[\mathbf{Fisher}_{k-1}^{n}+\boldsymbol{D}^{11}\left(\boldsymbol{X}_{k-1}^{n}\right)\right]^{-1}\boldsymbol{D}^{12}\left(\boldsymbol{X}_{k-1}^{n}\right)+\boldsymbol{G}_{k}^{n}, \tag{S5}$$

with

$$\begin{cases}\boldsymbol{D}^{11}\left(\boldsymbol{X}_{k-1}^{n}\right)=E\left[-\Delta_{\boldsymbol{X}_{k-1}}^{\boldsymbol{X}_{k-1}}\ln p\left(\boldsymbol{X}_{k}^{n}\mid\boldsymbol{X}_{k-1}^{n}\right)\right],\\ \boldsymbol{D}^{12}\left(\boldsymbol{X}_{k-1}^{n}\right)=E\left[-\Delta_{\boldsymbol{X}_{k-1}}^{\boldsymbol{X}_{k}}\ln p\left(\boldsymbol{X}_{k}^{n}\mid\boldsymbol{X}_{k-1}^{n}\right)\right],\\ \boldsymbol{D}^{21}\left(\boldsymbol{X}_{k-1}^{n}\right)=E\left[-\Delta_{\boldsymbol{X}_{k}}^{\boldsymbol{X}_{k-1}}\ln p\left(\boldsymbol{X}_{k}^{n}\mid\boldsymbol{X}_{k-1}^{n}\right)\right],\\ \boldsymbol{D}^{22}\left(\boldsymbol{X}_{k-1}^{n}\right)=E\left[-\Delta_{\boldsymbol{X}_{k}}^{\boldsymbol{X}_{k}}\ln p\left(\boldsymbol{X}_{k}^{n}\mid\boldsymbol{X}_{k-1}^{n}\right)\right],\\ \boldsymbol{G}_{k}^{n}=E\left[-\Delta_{\boldsymbol{X}_{k}}^{\boldsymbol{X}_{k}}\log p\left(\boldsymbol{Z}_{k}^{m,n}\mid\boldsymbol{X}_{k}^{n}\right)\right],\end{cases} \tag{S6}$$

where symbol Δ indicates the second-order partial derivative and $\boldsymbol{G}_{k}^{n}$ is the information gain obtained by sensor measurement.

For the Gaussian systems, Eq. (S6) can be written as

$$\begin{cases}\boldsymbol{D}^{11}\left(\boldsymbol{X}_{k-1}^{n}\right)=\left(\boldsymbol{F}_{\eta_k}^{n}\right)^{\mathrm{T}}\left(\boldsymbol{Q}_{\eta_k}^{n}\right)^{-1}\boldsymbol{F}_{\eta_k}^{n},\\ \boldsymbol{D}^{12}\left(\boldsymbol{X}_{k-1}^{n}\right)=\left[\boldsymbol{D}^{21}\left(\boldsymbol{X}_{k-1}^{n}\right)\right]^{\mathrm{T}}=-\left(\boldsymbol{F}_{\eta_k}^{n}\right)^{\mathrm{T}}\left(\boldsymbol{Q}_{\eta_k}^{n}\right)^{-1},\\ \boldsymbol{D}^{22}\left(\boldsymbol{X}_{k-1}^{n}\right)=\left(\boldsymbol{Q}_{\eta_k}^{n}\right)^{-1},\\ \boldsymbol{G}_{k}^{n}=\rho\left(\boldsymbol{J}_{k}^{m,n}\right)^{\mathrm{T}}\left(\boldsymbol{O}^{\boldsymbol{m}}\right)^{-1}\left(\boldsymbol{J}_{k}^{m,n}\right),\end{cases} \tag{S7}$$

where $\boldsymbol{J}_{k}^{m,n}$ is the Jacobian matrix of $\boldsymbol{h}^{m}\left(\boldsymbol{X}_{k}^{n}\right)$ mentioned in Eq. (22) and $\boldsymbol{O}^{m}$ is the measurement-error matrix of sensor *m*. Note that the actual motion model of target *n* cannot be obtained in sensor scheduling, so we use the model with the maximum probability in model set $\boldsymbol{\eta}_{\mathrm{model},k}^{n}$ as the actual motion model, that is, $\eta_k=\underset{i=1,2....,\eta_{\mathrm{total}}}{\arg\max}\,\mu_k^i$ (Xu et al., 2019).

References

Kirubarajan T, Bar-Shalom Y, 2003. Tracking evasive move-stop-move targets with a GMTI radar using a VS-IMM estimator. *IEEE Trans Aerosp Electron Syst*, 39(3):1098-1098. https://doi.org/10.1109/TAES.2003.1238762

Song D, Tharmarasa R, Florea MC, et al., 2019. Multi-vehicle tracking with microscopic traffic flow model-based particle filtering. *Automatica*, 105(1):28-35. https://doi.org/10.1016/j.automatica.2019.03.016

Xu GG, Shan GL, Duan XS, 2019. Non-myopic scheduling method of mobile sensors for manoeuvring target tracking. *IET Radar Sonar Navig*, 13(11):1899-1908. https://doi.org/10.1049/iet-rsn.2019.0178

Yu M, Oh H, Chen W, 2016. An improved multiple model particle filtering approach for manoeuvring target tracking using airborne GMTI with geographic information. *Aerosp Sci Technol*, 52(5):62-69. https://doi.org/10.1016/j.ast.2016.02.016